

Original Article

Investigation on elastic properties and radiation shielding of lead-recycled cathode ray tube glass system

Raewat Laopaiboon, Katayut Wichai, Sukhon Khottham,
Jintana Laopaiboon, and Oruethai Jaiboon*

*Department of Physics, Faculty of Science,
Ubon Ratchathani University, Warin Chamrap, Ubon Ratchathani, 34190 Thailand*

Received: 18 January 2019; Revised: 26 March 2019; Accepted: 2 April 2019

Abstract

The elastic and radiation shielding properties of lead-recycled cathode ray tube (CRT) glass were investigated in order to study the possible reduction in the use of toxic lead oxide glass by partial replacement using CRT glass waste. The elastic properties of lead-recycled glass were studied using the pulse-echo ultrasonic technique and it was found that the elastic properties varied with CRT content in the glass. This indicated the existence of some modifying cations in the CRT. The radiation shielding properties of the glass were also studied by means of the calculated mass attenuation coefficient, mean free path, and half-value layer using the WinXCom program. The addition of CRT glass was found to deteriorate the radiation shielding properties of lead glass. However, lead-recycled CRT glass still exhibited better radiation shielding properties than the conventional barite concrete. Therefore, lead-recycled CRT glass can be a potential candidate for radiation shielding applications.

Keywords: lead oxide glass, cathode ray tube, recycled glass, elastic moduli, radiation shielding material

1. Introduction

With the significant advances in the development of display technology of television, Cathode Ray Tube (CRT) monitor was displaced by Liquid Crystal Display (LCD), Plasma Display Panel (PDP) and display made of Organic Light Emitting Diode (OLED) (Poon, 2008; Andreola, Barbieri, Corradi, & Lancellotti, 2007). These new television displays can realize the higher definition image, lower energy consumption and reduced eyestrain issue. Therefore, instead of repairing or reusing, many CRT monitors have been discarded as Electronic-Waste (E-Waste). This E-Waste includes a term for electronic products that have become unwanted, out-of-date and non-working. The CRT monitor is usually made up of 4 types of glass components (panel, cone, and neck and frit junction) and these CRT glass components can be accounted for 50% to 85% of the total weight of CRT

monitor (Jaeger, 1975; Zughbi, Kharita, & Shehada, 2017; Xing *et al.*, 2018). For electronic radiation protection purposes, some heavy metals (e.g. lead, barium and strontium) were added during manufacturing process of these CRT glass components. Cone and neck glasses at least contain high amount of lead (Pb) and panel glass contains barium (Ba) and strontium (Sr) (Andreola, Barbieri, Corradi & Lancellotti, 2007; Hui & Sun, 2011). Because of high toxicity of these heavy metals, especially lead (Pb), waste management of discarded CRT glass has become a global environment problem (Hui & Sun, 2011; Socolof, Overly & Geibig, 2005; Andreola, Barbieri, Corradi & Lancellotti, 2007). In Thailand, disposal of CRT waste is rising sharply. It was predicted that in 2010 about 1.5 million televisions and 1.5 million computers were discarded improperly by burying them (Sua-iam & Makul, 2013; Rahad, 2015). Toxic metal can leach into the ground and effect environment and human health. In order to reduce the disposal of CRT glass, many researchers have tried to reuse and recycle them such as the use of crushed discarded-CRT glass in many types of concrete such as barite concrete (Ling & Poon, 2012; Zhao, Poon & Ling, 2013; Ling & Poon, 2014). Some researchers has tried to use this concrete

*Corresponding author

Email address: oruethai.j@ubu.ac.th

as radiation shielding material however there are many unavoidable disadvantages: (1) Generally, after prolonged exposure to nuclear radiation, formation of crack occurs in concrete due to arising of tensile stress from volume change when undergoes shrinkage, settlement, thermal stress, hydration heat, weather and load, (2) After absorption of radiation, concrete becomes hot and loss of water can occurs, this lead to an uncertainty in its shielding properties, and (3) This shielding concrete is opaque so it is impossible to see inside the shielding area (Kaundal, Kuar, Singh & Singh, 2010; Singh, Kaur & Kuandal, 2014). From the limitations of concrete a, glass researchers has utilized the transparent metal oxide glass as radiation shielding materials. It was found that one of the excellent radiation shielding glass is lead oxide glass, which can be used as X-ray observation equipment (Kaundal, 2016). However, lead oxide is toxic to environment.

This research aimed to reduce the use of lead oxide by partial replacement with CRT glass waste. At first, the chemical composition of the glass components of a CRT monitor were analyzed and then mixed with lead oxide (Pb_3O_4) during the manufacturing process. After that the elastic properties of the lead-recycled CRT glass were investigated using the pulse-echo ultrasonic technique. Moreover, the radiation shielding properties were evaluated by the WinXcom program and compared with the standard nuclear radiation shielding concrete (i.e., barite concrete).

2. Materials and Methods

2.1 CRT preparation and characterization

The CRT glass for this research was acquired from the display components of desktop computer monitors. The CRT glass was crushed into a fine powder using a mortar. The elemental analysis of CRT glass was conducted using energy dispersive X-ray spectroscopy (EDS) (Table 1). The analysis revealed significant amounts of oxygen (O) and silicon (Si) with small amounts of Ba, sodium (Na), potassium (K), Pb, calcium (Ca), aluminum (Al), and magnesium (Mg).

2.2 Lead-recycled CRT glass preparation

The glass system of (x)CRT-(100-x)PbO glass, where $x = 0, 10, 20, 30,$ and 40 mol%, were prepared by the conventional melt quenching method. The mixture of crushed CRT glass and Pb_3O_4 were melted in ceramic crucibles at around $1,250$ °C. After 2 h of the melting process, the molten glass was quickly poured into warmed stainless steel molds and annealed at 540 °C for 2 h, followed by slow cooling to room temperature. The samples of lead-recycled CRT glass were then cut, ground and polished to obtain flat, parallel end faces for ultrasonic velocity measurement with straight and angle beam probes.

2.3 Density and molar volume

Archimedes' principle was applied to determine the density at room temperature of the lead-recycled CRT glass using n-hexane as the immersion liquid. The density was calculated using Equation 1 (Gaafar & Marzonk, 2007):

$$\rho = \rho_{im} \left(\frac{W_{air}}{W_{air} - W_{im}} \right) \quad (1)$$

where ρ_{im} is the density of the immersion liquid at room temperature and W_{air} and W_{im} are the weights of the lead-recycled CRT glass in air and in the immersion liquid, respectively.

The molar volume (V_m) of the lead-recycled CRT glass can be determined from Equation 2 (Laopaiboon, Bootjomchai, Chanphet, & Laopaiboon, 2011):

$$V_m = \frac{M}{\rho} \quad (2)$$

where M is the molecular weight of the lead-recycled CRT glass. All measurements were repeated three times for accuracy.

2.4 Ultrasonic velocity measurement and elastic properties analysis

The velocities of ultrasonic wave in lead-recycled CRT glass were evaluated using the pulse-echo technique at 4 MHz with ULTRAGEL II (MAGNAFLUX) as a couplant. The elapsed time between the transmitter and the receiver of the pulse was measured and then used to calculate the ultrasonic velocities using Equation 3 (El-Mallawany, El-Khoshkhany, & Afifi, 2006; Marzouk & Gaafar, 2007):

$$v = \frac{2x}{\Delta t} \quad (3)$$

where x is the thickness (cm) of the sample and Δt is the time interval (s^{-1}).

Longitudinal and shear ultrasonic velocities (v_l and v_s , respectively) and density (ρ) of the glass samples were then applied to calculate the elastic moduli, Poisson's ratio, and microhardness using Equations 4 through 8 (Afifi & Marzonk, 2003).

$$\text{Longitudinal modulus: } L = \rho v_l^2 \quad (4)$$

$$\text{Shear modulus: } G = \rho v_s^2 \quad (5)$$

$$\text{Bulk modulus: } K = L - \left(\frac{4}{3}\right)G \quad (6)$$

$$\text{Young's modulus: } E = 2(1 + \sigma)G \quad (7)$$

Table 1. Chemical analysis of CRT glass by the EDS technique.

Element	O	Si	Ba	Na	K	Pb	Ca	Al	Mg	Total
wt%	36.08	31.75	8.29	7.57	6.08	6.02	1.80	1.70	0.70	100

$$\text{Poisson's ratio: } \sigma = \frac{L-2G}{2(L-G)} \quad (8)$$

$$\text{Microhardness: } H = \frac{(1-2\sigma)E}{6(1+\sigma)} \quad (9)$$

2.5 Structural analysis by Fourier transform infrared (FTIR) spectroscopy

Structure of the lead-recycled CRT glass was also analyzed using FTIR spectroscopy. The standard KBr pellet-preparing methods were applied. Then FTIR transmission spectra were recorded in the wavenumber range of 1200–400 cm^{-1} .

2.6 Shielding properties analysis

The radiation shielding properties of the lead-recycled CRT glass were evaluated by means of mass attenuation coefficient (μ_m), mean free path (mfp), and half-value layer (HVL). The mass attenuation coefficient for the selected radiation energies of 662, 1173, and 1332 keV (which represent the radiation from the radioisotopes of ^{137}Cs and ^{60}Co) was evaluated using the WinXCom program developed by the National Institute of Standards and Technology. Based on the mixture rule, the μ_m for a mixture of elements can be written as

$$\mu_m = \sum w_i(\mu/\rho)_i \quad (10)$$

where w_i and $(\mu/\rho)_i$ are the weight fractions and mass attenuation coefficients of the constituent elements, respectively (Gerward, Guilbert, Jensen, & Leyring, 2001, 2004). Then the μ_m of the lead-recycled CRT glass was used to calculate its mfp and HVL using Equations 11 and 12 (Bootjomchai, Laopaiboon, Yenchai, & Laopaiboon, 2012):

$$mfp = 1/\mu_m \quad (11)$$

$$HVL = 0.693/\mu_m \quad (12)$$

The calculated mfp and HVL were then compared to the conventional barite concrete.

3. Results and Discussion

3.1 Density and molar volume

The variations in the experimental values of density and molar volume with CRT content are shown in Figure 1. It can be seen that by increasing the CRT content, the density of the lead-recycled glass decreased. The decreased density can be explained by the fact that the atomic mass values of Si (28.08 g/mol), Na (22.98 g/mol), Mg (24.30 g/mol), Al (26.98 g/mol), K (39.09 g/mol), Ca (40.07 g/mol), and Ba (137.32 g/mol) of the CRT glass were all lower than Pb (207.2 g/mol). Figure 1 also shows a linear decrease of molar volume of the glass with increasing CRT glass concentration. Generally, a reduction in molar volume indicates a decrease in atomic spacing between atoms (Singh & Singh, 2013). This can be used to explain the decrease of molar volume of the lead glass with the addition of CRT glass since the ionic radius of Si^{4+}

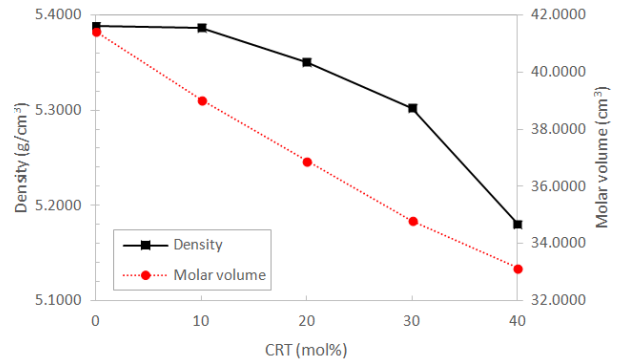


Figure 1. Variation of density and molar volume of lead-recycled CRT glass as a function of CRT content.

(0.54Å), which is the main cation from CRT glass, is much smaller than Pb^{4+} (1.19Å).

3.2 Ultrasonic velocity

In general, the change in ultrasonic velocities relates to a change in the number of non-bridging oxygen (NBO) atoms. In other words, it relates to a change in connectivity of the glass network. Therefore, the ultrasonic velocities reveal the degree of structural change in the glass (Bootjomchai, Laopaiboon, Yenchai & Laopaiboon, 2012). Figure 2 shows the longitudinal and shear ultrasonic velocities (v_l and v_s) in the lead-recycled CRT glass with different CRT glass contents. Generally, the addition of CRT glass leads to a change in both ultrasonic velocities which indicates a change in the number of NBO atoms in the glass network. With the small addition of only 10 mol% of CRT glass, both velocities decreased which possibly implied additional cations from the CRT glass into the lead glass network by breaking some of the Pb–O–Pb bonds. However, a further increase in CRT glass content to 20 and 30 mol% resulted in an increase of the velocities which showed the creation of a glass network with network bonding such as O–Si–O. Both velocities decreased again when the content of CRT glass increased further up to 40%. This revealed a breakdown of the glass network again when the concentration of CRT glass was higher. Therefore, the results from the ultrasonic velocity measurements exhibited a change in the glass network by insertion of cations (e.g., Si^{4+} and Mg^{2+}) from the CRT glass.

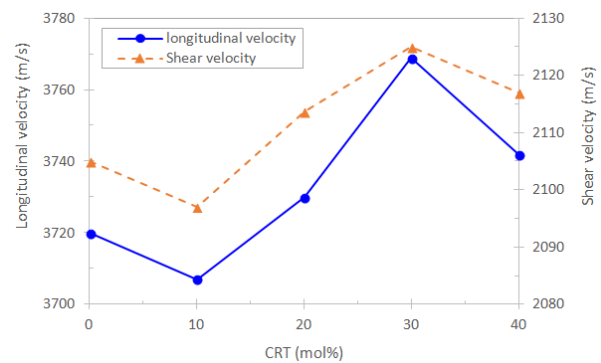


Figure 2. Variation of longitudinal and shear ultrasonic velocity in lead-recycled CRT glass as a function of CRT content.

3.3 Elastic properties

The elastic properties of the lead-recycled CRT glass were observed from the longitudinal modulus (L), shear modulus (G), bulk modulus (K), Young's modulus (E), Poisson's ratio (σ) and microhardness (H). The formulas used for the calculations are given in Equations 4 through 9. From the formulas, it can be expected that the factors that influenced the ultrasonic velocities in the glass also affected its elastic moduli. It was found from Figures 3a, 3b, and 3c that the values of longitudinal, shear, and Young's moduli were found to decrease with the addition of only 10 mol% of CRT glass. This can be attributed to the breakdown of the glass structure. However, when the addition of CRT increased to 20 mol%, these moduli rose. The increase in these moduli may be ascribed to the effect of the stronger field strength of the silicon cations (e.g., Si^{4+}) from the CRT glass (Du, 2009). This implies the presence of O-Si-O bonds in the glass structure. Then a further increase of CRT glass up to 30 mol% resulted in a reduction in these moduli, which disagreed with the results from the ultrasonic velocity measurements. Therefore, this decrease in the moduli with an increase in ultrasonic velocities can be attributed to the competition between the decrease of density and the rising in field strength of the silicon cations. When the CRT glass content increased to 40%, a further decrease of the moduli was observed. This indicated further reductions in the moduli due to the breakdown of the glass structure again. The bulk modulus, which describes the resistance to deformation of a material under pressure at all surfaces, showed a slightly different trend (Figure 3d). With the small addition of 10 mol% of CRT glass, the bulk modulus decreased. This may imply that the oxygen bonds in the lead glass structure were destroyed by the cations from the CRT glass, thereby creating NBO atoms.

This resulted in the formation of an open structure characterized by many open spaces (Marzouk, 2010). With further addition of CRT glass from 10 to 30 mol%, an increase in the bulk modulus was observed which indicated a more compact structure. This more compact structure could be attributed to a reduction in NBO atoms by formation of oxygen bonding with silicon cations as well as filling up open spaces by silicon cations. However, the addition of more CRT glass to 40 mol% sharply reduced the bulk modulus again which possibly implied the breakdown of the glass structure again (Sidek, Bahari, Halimah, & Yunus, 2012).

Poisson's ratio of the lead-recycled CRT glass also changed with the content of CRT glass (Figure 4 a). This observation lends support to the view that there is a change in the cross-link density with the addition of the CRT glass since it is well known that a change in the cross-link density results in an altered Poisson's ratio. Generally, Poisson's ratio of glass with a high cross-link density is in the range 0.1 to 0.2 while glass with a low cross-link density exhibits a Poisson's ratio between 0.3 and 0.5 (Rajendran, Palanivelu, Chauduri, & Goswami, 2003). In this present study, Poisson's ratio was lower than 0.3 which suggested a high cross-link density of our lead-recycled CRT glass. The rise in Poisson's ratio when the addition of CRT was only 10 mol% indicated a reduction in the cross-link density due to the breakdown of the glass network. When the addition of CRT increased to 20 mol%, Poisson's ratio decreased which implied an increase in the cross-link density due to the insertion of cations into the glass network with lower atomic packing density. However, when the CRT glass content was increased further to 30 mol%, Poisson's ratio surprisingly and largely increased again which implied a higher atomic packing density. This exhibited a stronger influence of filling up the free spaces by the silicon cations rather than the formation of O-Si-O in the glass

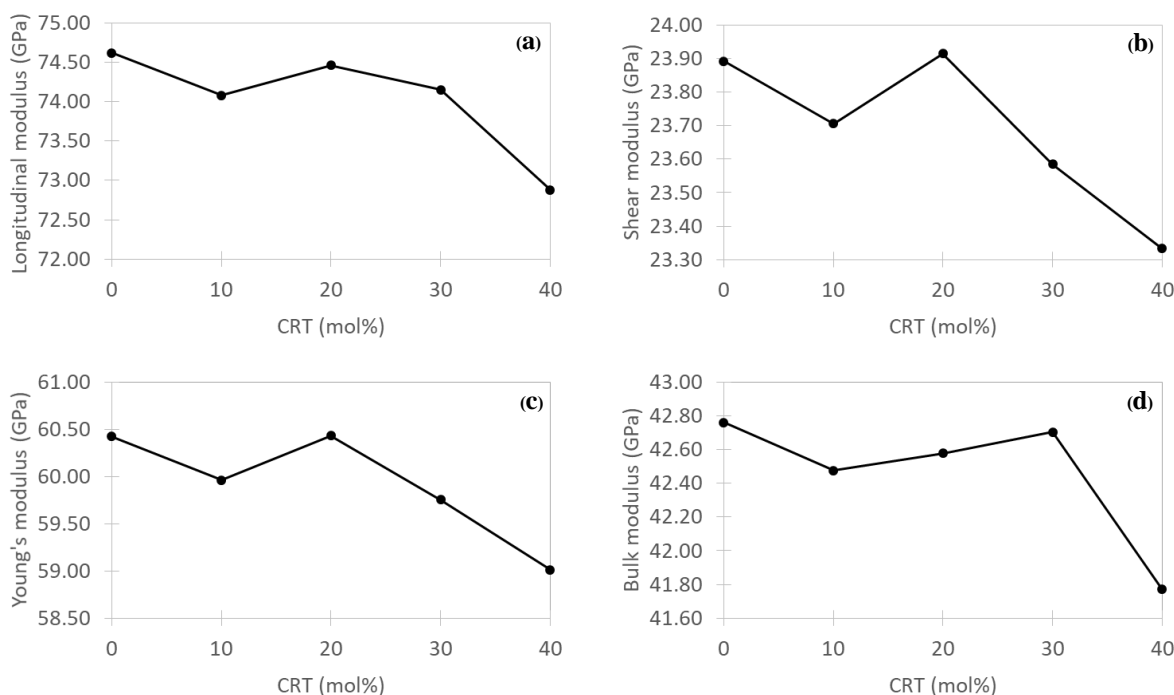


Figure 3. Variation of longitudinal (a), shear (b), Young's (c) and bulk (d) moduli of lead-recycled CRT glass as a function of CRT content.

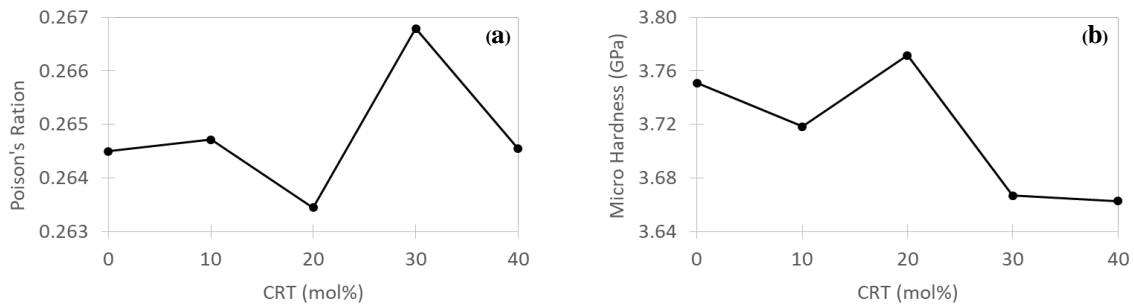


Figure 4. Variation of Poisson's ratio (a) and microhardness (b) of lead-recycled CRT glass as a function of CRT content.

network. Therefore, when the CRT glass concentration increased to 40 mol%, Poisson's ratio drops again which implied an increase of free space due to an influential breakdown of the glass structure (Rouxel *et al.*, 2008). This means that when most of the free space is filled, the addition of more silicon cations leads to a breakdown of the glass structure again.

Microhardness describes the stress required to eliminate the free volume of the glass. It was observed that the microhardness changed with the concentration of CRT glass (Figure 4b). The addition of 10 mol% CRT resulted in a decrease in the microhardness of the glass due to a breakdown of the glass structure. When the CRT glass content increased to 20 mol%, the maximum microhardness was reached. This indicated a strengthening of the lead-recycled CRT glass due to an introduction of stronger ionic bonding (e.g., O–Si–O) in the lead-glass structure. However, with further addition of more CRT glass, the microhardness of the lead-recycled glass decreased, which could be attributed to an influence of the large decrease in density due to the substitution of Pb^{4+} by Si^{4+} .

Therefore, all results from the ultrasonic measurements suggested that the addition of CRT glass led to a dimensional change in the glass structure and also a change in the cross-link density (Rajendran, Palanivelu, Chauduri & Goswami, 2003).

3.4 Structural analysis by FTIR spectroscopy

The FTIR transmission spectra can be divided into 2 active regions: (Region 1) 400–600 cm^{-1} is related to the bending vibration of Si–O–Si of SiO_4 (440–460 cm^{-1}) and the stretching vibration of Pb–O–Pb of PbO_4 (498–507 cm^{-1}) and (Region 2) 800–1200 cm^{-1} can be attributed the presence of a Si–O–NB asymmetrical vibration mode (850–1200 cm^{-1}) and Pb–O asymmetrical bending vibration mode (1090 cm^{-1}) (Bosca, Pop, Pascuta, & Culea, 2009; MacDonals, Schardt, Masiello, & Simmons, 2000; Rada, Dehelean, & Culea, 2011; Ramadevudu *et al.*, 2012; Rao *et al.*, 2012).

When the addition of CRT glass content was 10%, the intensity of the obvious peaks in Region 1 decreased but the intensity of the broad peaks in Region 2 increased (Figure 5). This implied the formation of NBO atoms by breaking down the Pb–O–Pb bonding and the formation of asymmetric Pb–O bonds. However, with a further addition of CRT glass content to 20%, the intensity of the peaks in Region 1 grew back and the disappearance of IR peaks in Region 2 was observed. This was possibly related to a reduction of NBO atoms by the formation of O–Si–O in the glass network.

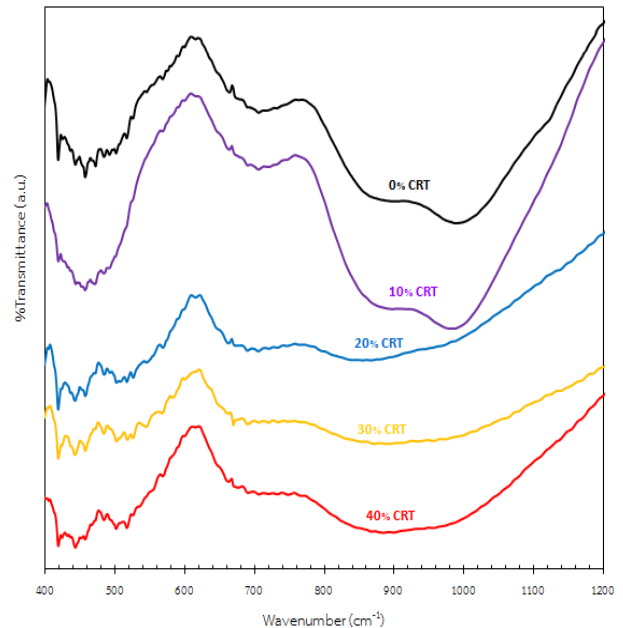


Figure 5. FTIR spectra of lead-recycled CRT glass.

However, with the further increase of CRT glass content to 30%, no significant difference was detected which implied insignificant formation of more O–Si–O bonds. Therefore, the excess cations from the CRT glass mainly filled up the free spaces in the glass structure. When the addition of CRT glass increased to 40%, the decrease of IR peaks in Region 1 with a presence of indistinct peaks in Region 2 suggested the formation of a few NBO atoms again. This observation was also consistent with the variation in ultrasonic velocities.

3.5 Radiation shielding properties

The mass attenuation coefficient (μ_m), mean free path (*mfp*), and half-value layer (*HVL*) are important parameters to estimate the radiation shielding properties of glass systems (Kaur, Singh, & Anand, 2015). The values of μ_m at radiation energies of 662, 1173, and 1332 keV were calculated using the WinXCom program. Figure 6 exhibits the variation of μ_m as a function of CRT glass content for all radiation energies. It was found that the μ_m values slightly decreased with the increments of CRT content. This can be explained by a decrease in densities of the lead-recycled CRT glass. Therefore, for all radiation energies, the addition of CRT glass

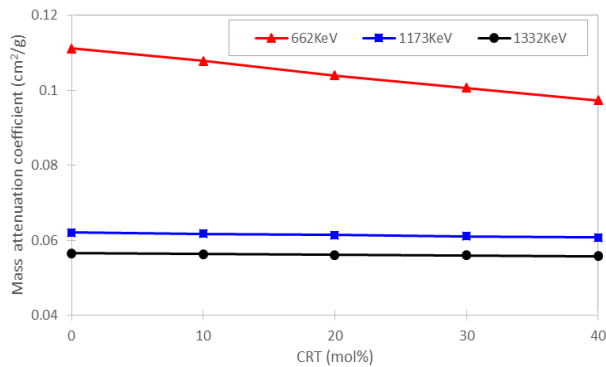


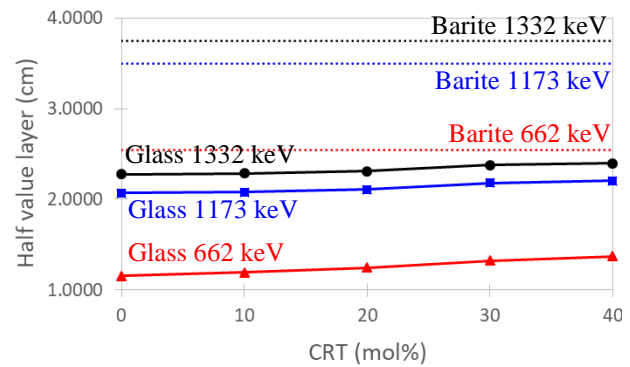
Figure 6. Variation of mass attenuation coefficient of lead-recycled CRT glass as a function of CRT content.

to lead-glass only resulted in a small reduction in the shielding properties (Kaur, Singh, & Pandey, 2014).

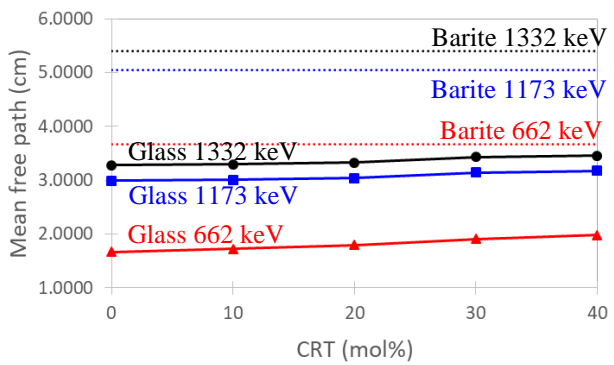
Variations of the mean free path (mfp), which is the reciprocal of measured linear attenuation coefficient, were observed in the lead-recycled CRT glass as a function of CRT content (Figure 7a). It can also be observed that the calculated mfp increased slightly as the CRT glass content increased. This indicated that as the CRT glass content increased, a longer distance was required to suppress and attenuate the incident radiation. Therefore, as the concentration of CRT glass increased, the shielding properties of the lead-recycled CRT glass became poorer. Nevertheless, we compared the mfp value of lead-recycled CRT glass with the conventional barite concrete. It was found that the mfp value of the lead-recycled CRT glass was lower than the barite concrete which indicated better shielding properties of the lead-recycled CRT glass than the barite concrete for all radiation energies. The half-value layer (HVL), which is the thickness of material where the intensity of radiation passing through it is decreased by 50%, of the lead-recycled CRT glass as a function of CRT content is shown in Figure 7b. The HVL was observed to slightly increase as the CRT glass content increased for all radiation energies. This increase in the HVL indicated a reduction in the shielding properties of the lead-recycled CRT glass in terms of thickness requirement. However, it was also found that the HVL values of the lead-recycled CRT glass were all lower than the barite concrete which indicated better shielding properties of the lead-recycled CRT glass for all radiation energies. Therefore, by means of mfp and HVL , the lead-recycled CRT glass has the potential to offer better radiation shielding compared to barite concrete.

4. Conclusions

Lead-recycled CRT glass was prepared from mixtures of crushed CRT and Pb_3O_4 using conventional melt quenching methods. The properties of the lead-recycled CRT glass were studied as a function of CRT content. It was found that the density and molar volume of lead-recycled CRT glass decreased as the CRT glass content increased which indicated partial substitution of the lead oxide network by cations, such as Si^{4+} , from the CRT glass. The elastic properties of the lead-recycled CRT glass were investigated using the pulse-echo ultrasonic technique. Variations in both longitudinal and shear ultrasonic velocities as a function of CRT glass content were



(a)



(b)

Figure 7. Variation of mean free path (a), and half-value layer (b) of lead-recycled CRT glass as a function of CRT content.

also observed. This revealed that the addition of cations in the CRT glass led to a change in network structure of the glass. The network-modifying cations broke down the $Pb-O-Pb$ bonding which created NBO atoms and also formed $O-Si-O$ network bonding. Thus, the elastic moduli of the lead-recycled CRT glass were also found to vary with CRT content. The radiation shielding properties of the lead-recycled glass at radiation energies of 662, 1173, and 1332 keV were also studied by means of the calculated mass attenuation coefficient (μ_m), mean free path (mfp), and half-value layer (HVL) using the WinXCom program. It was found that as more CRT glass content was added, the shielding properties became poorer. However, when compared with the conventional barite radiation shielding concrete, the lead-recycled CRT glass exhibited better radiation shielding properties.

Acknowledgements

The authors would like to thank Dr. Ussadawut Patakum from MTEC for the analysis of the CRT glass by the EDS technique.

References

- Afifi, H., & Marzonk, S. (2003). Ultrasonic velocity and elastic moduli of heavy metal tellurite glasses. *Material Chemistry Physics*, 80(2), 517–523. doi:10.1016/S0254-0584(03)00099-3

- Andreola, F., Barbieri, L., Corradi, A., & Lancellotti, I. (2007). CRT glass state of the art. A case study: Recycling in ceramic glazes. *Journal of the European Ceramic Society*, 27(2-3), 1623-1629. doi:10.1016/j.jeurceramsoc.2006.05.009
- Bosca, M., Pop, L., Borodi, G., Pascuta, P., & Culea, E. (2009). XRD and FTIR structural investigations of erbium-doped bismuth-lead-silver glasses and glass ceramics. *Journal of Alloys and Compounds*, 479(1), 579-582. doi:10.1016/j.jallcom.2009.01.001
- Bootjomchai, C., Laopaiboon, J., Yenchai, C., & Laopaiboon, R. (2012). Gamma-ray shielding and structural properties of barium-bismuth-borosilicate glasses. *Radiation Physics Chemistry*, 81(7), 785-790. doi:10.1016/j.radphyschem.2012.01.049
- Du, J. (2009). Molecular dynamics simulations of the structure and properties of low silica Yttrium Aluminosilicate Glasses. *Journal of the American Ceramic Society*, 92(1), 87-95. doi:10.1111/j.1551-2916.2008.02853.x
- El-Mallawany, R., El-Khoshkhany, N., & Afifi, H. (2006). Ultrasonic studies of $(\text{TeO}_2)_{50}-(\text{V}_2\text{O}_5)_{50-x}(\text{TiO}_2)_x$ glasses. *Material Chemistry Physics*, 95(2-3), 321-327. doi:10.1016/j.matchemphys.2005.06.025
- Gaafar, M.S., & Marzouk, S.Y. (2007). Mechanical and structural studies on sodium borosilicate glasses doped with Er_2O_3 using ultrasonic velocity and FTIR spectroscopy. *Physica B*, 388(1-2), 294-302. doi:10.1016/j.physb.2006.06.132
- Gerward, L., Guilbert, N., Jensen, K.B., & Levring, H. (2001). X-ray absorption in matter. Reengineering XCOM. *Radiation Physics Chemistry*, 60(1-2), 23-24. doi:10.1016/S0969-806X(00)00324-8
- Gerward, L., Guilbert, N., Jensen, K. B., & Levring, H. (2004). WinXCom—a program for calculating X-ray attenuation coefficients. *Radiation Physics Chemistry*, 71(3), 653-654. doi:10.1016/j.radphyschem.2004.04.040
- Hui, Z., & Sun, W. (2011). Study of properties of mortar containing cathode ray tubes (CRT) glass as replacement for river sand fine aggregate. *Construction and Building Materials*, 25, 4059-4064. doi:10.1016/j.conbuildmat.2011.04.043
- Jaeger, R. G. (1975). *Engineering Compendium on Radiation Shielding*. Vienna, Austria: Springer-Verlag.
- Kaundal, R. S., Kaur, S., Singh, N., & Singh, K. J. (2010). Investigation of structural properties of lead strontium borate glasses for gamma-ray shielding applications. *Journal of Physics and Chemistry of solid*, 71(9), 1191-1195. doi:10.1016/j.jpics.2010.04.016
- Kaundal, R. S. (2016). Comparative study of radiation shielding parameters for Bismuth Borate glasses. *Materials Research*, 19(4), 776-780. doi:10.1590/1980-5373-MR-2016-0040
- Kaur, K., Singh, K. J., & Anand, V. (2015). Correlation of gamma ray shielding and structural properties of $\text{PbO-BaO-P}_2\text{O}_5$ glass system. *Nuclear Engineering and Design*, 285, 31-38. doi:10.1016/j.nucengdes.2014.12.033
- Kaur, R., Singh, S., & Pandey, O. P. (2014). Structural variation in gamma ray irradiated $\text{PbO-Na}_2\text{O-B}_2\text{O}_3\text{-SiO}_2$ glasses. *Solid State Communication*, 188, 40-44. doi:10.1016/j.ssc.2014.02.022
- Laopaiboon, R., Bootjomchai, C., Chanphet, M., & Laopaiboon, J. (2011). Elastic properties investigation of gamma-radiated barium lead borosilicate glasses using ultrasonic technique. *Annals Nuclear Energy*, 38(11), 2333-2337. doi:10.1016/j.anucene.2011.07.035
- Ling, T. C. (2012). Feasible use of recycled CRT funnel glass as heavyweight fine aggregate in barite concrete. *Journal of Cleaner Production*, 33, 42-49. doi:10.1016/j.jclepro.2012.05.003
- Ling, T. C., & Poon, C. S. (2013). Use of recycled CRT funnel glass as fine aggregate in dry-mixed concrete paving blocks. *Journal of Cleaner Production*, 68, 209-215. doi:10.1016/j.jclepro.2013.12.084
- MacDonald, S. A., Schardt, C. R., Masiello, D. J., & Simmons, J. H. (2000). Dispersion analysis of FTIR reflection measurements in silicate glasses. *Journal of Non-Crystalline Solids*, 275(1-2), 72-82. doi:10.1016/S0022-3093(00)00121-6
- Marzouk, S. Y. (2010). The acoustic properties of borosilicate glass affected by oxide of rare earth gadolinium. *Physica B Condensed Matter*, 405(16), 3395-3400. doi:10.1016/j.physb.2010.05.011
- Marzouk, S. Y., & Gaafar, M. S. (2007). Ultrasonic study on some borosilicate glasses doped with different transition metal oxides. *Solid State Communication*, 144(10-11), 478-483. doi:10.1016/j.ssc.2007.09.017
- Poon, C. S. (2008). Management of CRT glass from discarded computer monitors and TV sets. *Waste Manage*, 28(9), 1499. doi:10.1016/j.wasman.2008.06.001
- Rada, S., Dehelean, A., & Culea, E. (2011). FTIR and UV-VIS spectroscopy investigations on the structure of the europium-lead-tellurate glasses. *Journal of Non-Crystalline Solids*, 357(16-17), 3070-3073. doi:10.1016/j.jnoncrsol.2011.04.013
- Rajendran, V., Palanivelu, N., Chauduri, B.K., & Goswami, K. (2003). Characterisation of semiconducting $\text{V}_2\text{O}_5\text{-Bi}_2\text{O}_3\text{-TeO}_2$ glasses through ultrasonic measurements. *Journal of Non-Crystalline Solids*, 320(1-3), 195-209. doi:10.1016/S0022-3093(03)00018-8
- Ramadevudu, G., Lakshmi, S., Rao, M., Shareeffuddin, M., Narasimha, C., & Lakshmiipathi, M. (2012). FTIR and optical absorption studies of new magnesium lead borate glasses. *Global Journal of Science Frontier Research Physics and Space Science*, 12(4). Retrieved from <https://www.researchgate.net/publication/232607201>
- Rao, T. G. V. M., Rupesh Kumar, A., Hanumantha Rao, B., Veeraiah, N., & Remi Reddy, M. (2012). Optical absorption, ESR, FT-IR spectral studies of iron ions in lead oxyfluoro silicate glasses. *Journal of Molecular Structure*, 1021, 7-12. doi:10.1016/j.molstruc.2012.04.026
- Rashad, A. M. (2015). Recycled cathode ray tube and liquid crystal display glass as fine aggregate replacement in cementitious materials. *Construction and Building Materials*, 93, 1236-1248. doi:10.1016/j.conbuildmat.2015.05.004
- Rouxel, T., Ji, H., Keryvin, V., hammouda, T., & Yoshida, S. (2008). Poisson's ratio and the glass network topology-relevance to high pressure densification

- and indentation behavior. *Advanced Materials Research*, 39-40, 137-146. doi:10.4028/www.scientific.net/AMR.39-40.137
- Sidek, H., Bahari, H. R., Halimah, M. K., & Yunus, W. M. (2012). Preparation and Elastic Moduli of Germanate Glass Containing Lead and Bismuth. *International Journal of Molecular Sciences*, 13(4), 4632-4641. doi:10.3390/ijms13044632
- Singh, D. P., & Singh, G. P. (2013). Conversion of covalent to ionic behavior of $\text{Fe}_2\text{O}_3\text{-CeO}_2\text{-PbO-B}_2\text{O}_3$ glasses for ionic and photonic application. *Journal of Alloys Compounds*, 546, 224-228. doi:10.1016/j.jallcom.2012.08.105
- Singh, K. J., Kaur, S., & Kaundal, R. S. (2014). Comparative study of gamma ray shielding and some properties of $\text{PbO-SiO}_2\text{-Al}_2\text{O}_3$ and $\text{Bi}_2\text{O}_3\text{-SiO}_2\text{-Al}_2\text{O}_3$ glass system. *Radiation Physics and Chemistry*, 96, 153-157. doi:10.1016/j.radphyschem.2013.09.015
- Socolof, M. L., Overly, J. G., & Geibig, J. R. (2005). Environmental life-cycle impacts of CRT and LED desktop computer displays. *Journal of Cleaner Production*, 13(13-14), 1281-1294. doi:10.1016/j.jclepro.2005.05.014
- Sua-iam, G., & Makul, N. (2013). Use of limestone powder during incorporation of Pb containing cathode ray tube waste in self-compacting concrete. *Journal of Environmental Management*, 128, 931-940. doi:10.1016/j.jenvman.2013.06.031
- Xing, M., Wang, J., Fu, Z., Zhang, D., Wang, Y., & Zhang, Z. (2017). Extraction of heavy metal (Ba, Sr) and high silica glass powder synthesis from waste CRT panel glass by phase separation. *Journal of Hazardous Materials*, 347, 8-14. doi:10.1016/j.jhazmat.2017.12.046
- Zhao, H., Poon, C. S., & Ling, T. C. (2013). Utilizing recycled cathode ray tube funnel glass sand as river sand replacement in the high-density concrete. *Journal of Cleaner Production*, 51, 184-190. doi:10.1016/j.jclepro.2013.01.025
- Zughbi, A., Kharita, M. H., & Shehada, A. M. (2017). Determining optical and radiation characteristics of cathode ray tubes' glass to be reused as radiation shielding glass. *Radiation Physics and Chemistry*, 136, 71-74. doi:10.1016/j.radphyschem.2017.02.035